analytical chemistry

Article

pubs.acs.org/ac

A Simple Construction of Electrochemical Liver Microsomal Bioreactor for Rapid Drug Metabolism and Inhibition Assays

Charuksha Walgama,[†] Rajasekhara Nerimetla,[†] Nicholas F. Materer,[†] Deniz Schildkraut,[‡] James F. Elman,[‡] and Sadagopan Krishnan*[,†]

[†]Department of Chemistry, Oklahoma State University, Stillwater, Oklahoma 74078, United States

[‡]Filmetrics Application Lab—Rochester, 250 Packett's Landing, Fairport, New York 14450, United States

Supporting Information

ABSTRACT: In order to design a green microsomal bioreactor on suitably identified carbon electrodes, it is important to understand the direct electrochemical properties at the interfaces between various carbon electrode materials and human liver microsomes (HLM). The novelty of this work is on the investigation of directly adsorbed HLM on different carbon electrodes with the goal to develop a simple, rapid, and new bioanalytical platform of HLM useful for drug metabolism and inhibition assays. These novel biointerfaces are designed in this study by a one step adsorption of HLM directly onto polished basal plane pyrolytic graphite (BPG), edge plane pyrolytic graphite (EPG), glassy carbon (GC), or high-purity graphite (HPG) electrodes. The estimated direct electron transfer (ET) rate constant of HLM on the smooth GC surface was significantly greater than that of the other electrodes. On the other hand, the electroactive surface coverage and stability of microsomal films were greater on highly surface defective, rough EPG and HPG electrodes compared to the smooth GC and less defective hydrophobic BPG surfaces. The presence of significantly higher oxygen functionalities and flatness of the GC surface is attributed to favoring faster ET rates of the coated layer of thin HLM film compared to other electrodes. The cytochrome P450 (CYP)-specific bioactivity of the liver microsomal film on the catalytically superior, stable HPG surface was confirmed by monitoring the electrocatalytic conversion of testosterone to 6β-hydroxytestosterone and its inhibition by the CYP-specific ketoconazole inhibitor. The identification of optimal HPG and EPG electrodes to design biologically active interfaces with liver microsomes is suggested to have immense significance in the design of one-step, green bioreactors for stereoselective drug metabolite synthesis and drug metabolism and inhibition assays.

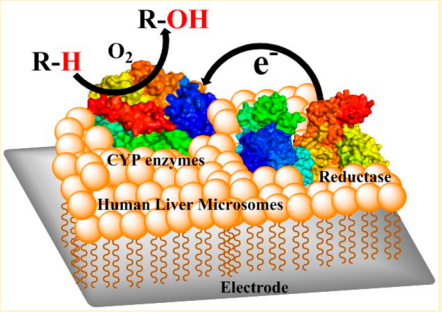

We demonstrate here for the first time that simple construction of bioactive interfaces of human liver fractions with electrodes has the potential to transform the current paradigm of drug development by providing rapid screening platforms for drug metabolism and inhibition. Human cytochrome P450s (CYPs) are the major drug metabolizing enzymes present in the liver. The remarkable and broad catalytic properties of CYPs suggest that they may prove useful in the stereoselective green syntheses of fine chemicals.[1,2] The *in vivo* catalytic activities of CYPs primarily depend on the electrons supplied by cytochrome P450-reductase (CPR) with NADPH acting as the electron source.[3] The significance of the CYP−CPR interaction in altering CYP enzyme turnover has been examined in several biochemical and electrochemical studies.[4−7] CPR contains both flavin adenine dinucleotide (FAD) and flavin mononucleotide (FMN) cofactors and is the only known membrane-bound flavoprotein. CPR transfers electrons from NADPH via FAD to FMN and further to the heme centers of CYPs. In this electron transfer (ET) pathway, phospholipid bilayers play a crucial role in modulating the redox potentials of FMN and FAD in CPR and aid in ET.[8]

In direct electrochemistry, the electrode acts as an electron donor to redox protein films under an applied negative potential.[9−11] Because purification of CYPs is a tedious process, the application of liver microsomes or genetically engineered supersomes (microsomes specifically enriched with a CYP enzyme and its reductase) containing CYPs in the development of new biosensing and electrocatalytic systems is an emerging research area.[7] Human liver microsomes (HLM) are obtained by homogenizing liver tissue in buffer and centrifuging the resulting slurry at 10 000*g* to specifically isolate the major membrane-bound drug metabolizing enzymes such as CYP enzymes and their redox partner protein, CPR. HLM are extensively used in pharmaceutical industries for *in vitro* drug metabolism and inhibition assays and for evaluating ADME (Absorption, Distribution, Metabolism, and Excretion) properties of any drug in development.[12] Direct ET and catalytic studies of genetically engineered microsomes,[13] rat liver microsomes,[14] and HLM[15] assembled as films with polyions, microsomes coated on different thiolated hydrophobic gold

Received: November 27, 2014
Accepted: April 12, 2015
Published: April 12, 2015

DOI: 10.1021/ac5044362
Anal. Chem. 2015, 87, 4712−4718

electrodes,[16] and layer-by-layer films of purified human CYPs and microsomal CPR[17] have been conducted.

Carbon electrodes are known for their robustness, inexpensive nature, ease of cleaning, and reusability. The objective of this study is to develop a suitable carbon electrode platform that will allow immobilization of complex HLM by direct adsorption with stability and bioactivity. Such an analytical platform is expected to offer a novel, rapid design of HLM electrodes for drug metabolism assays involving a simple and cost-effective electrochemical approach. We have chosen four commonly used carbon electrodes, basal-plane pyrolytic graphite (BPG), edge-plane pyrolytic graphite (EPG), glassy carbon (GC), and high purity graphite (HPG), in this study.

Considering the importance of HLM in pharmaceutical drug development and toxicology fields, the demonstration of a rapid, stable, and one-step microsomal bioreactor design for inexpensive electrochemical drug metabolism and inhibition assays is novel and highly significant. We additionally provide insights on the carbon-electrode-dependent direct electrochemical and electrocatalytic properties of adsorbed HLM.

EXPERIMENTAL SECTION

Materials and Reagents. HLM (total protein 20 mg mL^{-1}, total CYPs 0.5 nmol mg^{-1} protein, NADPH-cyt c reductase activity 154 nmol mg^{-1} protein min^{-1} that corresponds to 0.051 nmol CPR mg^{-1} protein,[18] and Cytochrome b_5 0.34 nmol mg^{-1} protein) were purchased from XenoTech (Lenexa, KS, USA) and used as received. Disk electrodes of EPG, BPG, HPG, and GC were used in this study [geometric area 0.2 cm^2]. Pure EPG and BPG disks were constructed from PG blocks (1 × 1 × 0.5 in., Momentive Performance Materials, Albany, NY, USA). Basal planes are present parallel to the PG surface, and edge planes are aligned perpendicular to the surface.[19] HPG disks were purchased from McMaster-Carr (POCO EDM-4 grade, Atlanta, GA, USA), and GC electrodes were obtained from CH Instruments (Austin, TX, USA). Testosterone, ketoconazole, and standard 6β-hydroxytestosterone were purchased from Sigma-Aldrich. All other reagents were high purity analytical grade. Unless otherwise specified, all electrochemical measurements were carried out in phosphate buffer containing 0.15 M NaCl, pH 7.0 at 25 °C.

Microsomal Film Preparation. Prior to use, all electrodes were polished and cleaned by following standard procedures to obtain fresh surfaces for adsorbing HLM. Briefly, BPG, EPG, and HPG disk electrodes were freshly polished using SiC paper (P320 grit), and GC electrodes were polished in an aqueous slurry of alumina (1 μm) placed on an alumina pad (EXTEC Corp., Enfield, CT, USA) to obtain fresh surfaces. The polished electrodes were cleaned by ultrasonication in water for 1 min and then dried under nitrogen. A film of HLM was formed on each freshly polished electrode by adsorption from a 10 μL solution of HLM for 20 min at 4 °C. The electrodes were rinsed with buffer to remove weakly and unbound HLM and then used for cyclic voltammetry (CV) studies.

Colorimetric Assay for Presence of Microsomal Films on Electrodes. The presence of phospholipids in the microsomal films immobilized on various electrode surfaces was confirmed using a colorimetric assay.[20] The major microsomal phospholipids, such as sphingomyelin, phosphatidyl serine, phosphatidyl ethanolamine, and lecithin, are the active components that form a red color complex with ammonium ferrothiocyanate that absorbs at ~488 nm in chloroform as a solvent.[20]

Fourier Transform Infrared (FTIR) Spectroscopy. The liver microsomal films on the electrodes were characterized by FTIR spectroscopy (Nicolet IS50 FTIR, Thermo Scientific) in the attenuated total reflectance mode (ATR). The electrodes were mounted on an ATR diamond crystal, and 64 scans were acquired and averaged to obtain a good signal-to-noise ratio. Similarly, the FTIR spectrum of HLM dry coated directly on an ATR diamond crystal was obtained for comparison.

Microscopic Characterization of the Electrodes. The surface morphologies of BPG, EPG, GC, and HPG disk electrodes before and after coating with a layer of HLM were characterized by scanning electron microscopy (SEM, Model: FEI Quanta 600FE). An accelerating voltage of 20 kV was applied. The images were acquired using the FEI xT Microscope Control Software.

Thickness of HLM Film on Different Electrodes. The dry film thicknesses of adsorbed microsomal films on BPG, EPG, GC, and HPG disk electrodes were measured by the spectral reflectance method using a Filmetrics F40 system (Fairport, NY, USA). Different locations along the microsomal films were scanned to obtain a range of thicknesses representative of the entire surface of each electrode. For each location, the thickness was calculated from the reflectance spectrum obtained at a normal incidence in the visible wavelength region. The refractive index of HLM was assumed to be 1.54 at 632.8 nm.[21] The experiment was repeated with three replicate samples of microsomal films for each type of electrode.

XPS Analysis. X-ray photoelectron spectroscopy (XPS) measurements were performed using the Mg anode of a PHI 300 W twin anode X-ray source and the PHI double-pass cylindrical mirror analyzer as the detector with a pass energy of 100 eV. The instrument comprised a surface analysis system with a base pressure of 2×10^{-10} Torr. General survey scans were carried out for polished GC, EPG, BPG, and HPG electrodes. Percentage amounts of C and O were calculated for comparison among electrodes.

Electrochemical Measurements. A CH instrument 6017E electrochemical analyzer was used for CV experiments. Measurements were made in a standard three-electrode cell consisting of an Ag/AgCl reference electrode (1 M KCl, CH Instruments), a Pt-wire counter electrode, and a HLM-coated working electrode disk (BPG, EPG, GC, or HPG). A 90% IR compensation was employed before starting the CV scans. For anaerobic CV experiments, the cell buffer was purged under high purity nitrogen for 30 min before acquiring voltammograms, and a constant nitrogen atmosphere was maintained during measurements.

Electrocatalytic Oxygen Reduction. Oxygen plays an important role in CYP enzyme-catalyzed reactions by aiding in the formation of the reactive CYP-ferryloxy radical cation [$^{+\bullet}$(CYP-Fe^{IV}=O)].[3] This oxoform is presumed to be the active oxidant of CYPs that can oxygenate a bound drug molecule or other compounds.[3,4] Oxygen binding to CYPs requires the initial reduction of the heme-cofactor of CYPs by CPR involving an *in vivo* electron donor (e.g., NADPH),[4] or it can be driven *in vitro* via the electrode by an applied potential.[7] The HLM catalyzed oxygen reduction was studied in stirred buffer solutions to achieve mass transfer by convection,[22] which provided better film stability than a rotating disk setup. Defined percentages of oxygen were mixed with nitrogen using two

DOI: 10.1021/ac5044362
Anal. Chem. 2015, 87, 4712−4718

mass flow controllers (Aalborg Instruments & Controls Inc., NY, USA) and supplied to the film of HLM on each electrode. The percentage O_2 was converted to the corresponding concentration using the Henry's law equation.[23,24]

Electrocatalytic Testosterone Hydroxylation and Liquid Chromatography Detection of Products. The electrocatalytic conversion of testosterone to 6β-hydroxytestosterone by the designed microsomal films was confirmed by liquid chromatography.[16,17] In brief, the electrodes adsorbed with HLM were placed in a stirred three-electrode microcell containing 250 μM testosterone in 1 mL of potassium phosphate buffer, pH 7.0. The electrolysis was carried out at an applied potential of −0.6 V vs Ag/AgCl for 1 h under a constant supply of oxygen. The reaction mixture was analyzed by high performance liquid chromatography (HPLC, C-18 Column, Shimadzu LCMS-2010EV). The product was identified using standard 6β-hydroxytestosterone (Sigma). For inhibition studies, 100 μM ketoconazole was added to 250 μM testosterone in a pH 7.0 buffer, electrolysis was carried out, and the reaction mixture was analyzed by HPLC. A gradient elution involving an acetonitrile/water solvent mixture was used in HPLC analysis: 10% acetonitrile for 0−10 min followed by 10−50% acetonitrile up to 60 min and a constant 50% acetonitrile until 80 min at a flow rate of 0.3 mL min^{-1}.

RESULTS AND DISCUSSION

Spectral, Spectroscopic, and Microscopic Characterization of Films of HLM on Electrodes. The formation of a red colored complex in the reaction of HLM with ammonium ferrothiocyanate (λ_{max} at 488 nm)[20] confirmed the presence of microsomal phospholipids in the adsorbed microsomal films (Figure S1). FTIR characterization of HLM on the various electrodes showed the presence of the amide I and amide II bands of microsomal proteins at 1650 and 1542 cm^{-1}, respectively (Figure S2). Additionally, the fundamental bond stretching frequencies of phospholipids in the vibrational region 1300−900 cm^{-1} were identified by the FTIR characterization.[20,25,26] The characteristic phospholipid vibrational bands were noted at 1237 (P═O), 1045 (P−O), 990 (P−O−C), and 924 cm^{-1} (C−N of choline group) for microsomal films coated on the electrodes (Figure S2). Similar vibrational bands were also noted for the HLM film coated directly on an FTIR-ATR crystal (Figure S2) confirming that the electrodes did not induce any notable change in the phospholipid structures of adsorbed HLM.

The scanning electron micrographs of polished GC, HPG, EPG, and BPG disk electrodes and those adsorbed with a layer of HLM are shown in Figure 1A−H. The GC surface is relatively smooth, whereas the EPG surface features large surface defects. The BPG surface displays relatively less surface defects,[19] and the HPG surface exhibits platelet-like surface defects that differ from pure edge and basal planes (Figure 1A−D, respectively). All observed surface morphologies of polished electrodes are in good agreement with results of prior studies.[27−30] Adsorption of a layer of HLM on each electrode changed the surface morphology and produced coated film textures, which confirmed the formation of microsomal films on the electrodes (Figures 1E−H).

Electrochemical Probing of Microsomal Film Voltammetry. To drive electrocatalysis of a drug conversion into metabolites, it is necessary that electrons are successfully delivered from the electrode to reduce the immobilized liver microsomal proteins. To examine this, we utilized cyclic

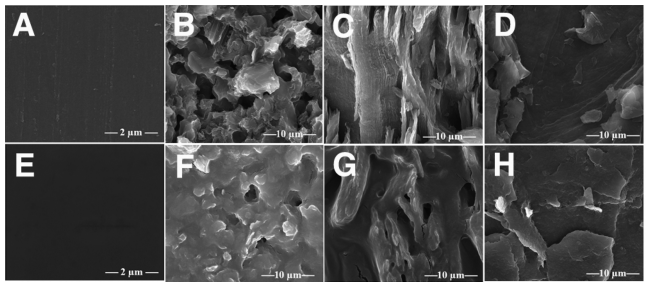

Figure 1. SEM images of polished (A) GC, (B) HPG, (C) EPG, and (D) BPG electrodes and these electrodes after being coated with a layer of HLM: (E) GC/HLM, (F) HPG/HLM, (G) EPG/HLM, and (H) BPG/HLM.

voltammetry to study the direct electron transfer properties of designed microsomal films on various carbon electrodes. Figure 2A shows the background subtracted cyclic voltammo-

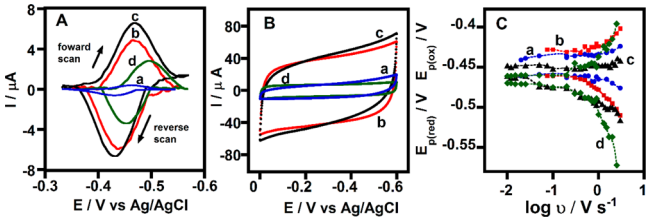

Figure 2. (A) Background subtracted cyclic voltammograms of liver microsomal films physisorbed on (a) GC, (b) HPG, (c) EPG, and (d) BPG electrodes at 0.7 V s^{-1} in anaerobic phosphate buffer, nitrogen atmosphere, pH 7.0, 25 °C. (B) The corresponding cyclic voltammograms (a−d) of control phosphatidylchloine films adsorbed similarly on the various electrodes. (C) Trumpet plots displaying the reduction and oxidation peak potentials of HLM films with logarithm of scan rate on (a) GC, (b) HPG, (c) EPG, and (d) BPG electrodes in anaerobic phosphate buffer, pH 7.0, 0.15 M NaCl, 25 °C.

grams of microsomal films adsorbed on the carbon electrodes in a nitrogen atmosphere at pH 7.0. Polished electrodes with an adsorbed phospholipid film (L-α-phosphatidylchloine) in the absence of microsomal proteins did not show any redox peaks (Figure 2B) and thus confirmed that the direct electron transfer from the electrode to microsomal proteins was achieved (Figure 2A). The peak separation between oxidation and reduction potentials with the logarithm of scan rate is shown in Figure 2C for the microsomal films on each electrode.

The average formal potential ($E^{\circ\prime}$) of microsomal films was in the range −0.45 to −0.47 V vs Ag/AgCl. The observed $E^{\circ\prime}$ values are in good agreement with prior reports on the formal potential of microsomal CPR protein.[14,15,17,31,32] On the other hand, purified CYPs (−0.3 to −0.33 V vs Ag/AgCl),[33] microsomal cyt b_5,[34] and only CYP-containing microsomes (−0.38 V vs Ag/AgCl)[16] are known to exhibit more positive formal potentials. Furthermore, the anaerobic peak potentials of microsomal films in nitrogen did not shift positive upon supplying carbon monoxide (Figure S3), which is against the characteristic feature of microsomal CYP enzymes.[33] This suggests that the observed voltammetric properties of microsomal films are characteristics of oxidoreductases in microsomes.[13−15]

The peak currents increased linearly with scan rates from 0.005 to 2 V s^{-1} for the immobilized microsomal films on all four carbon electrodes (Figure S4). This property confirms the

DOI: 10.1021/ac5044362
Anal. Chem. 2015, 87, 4712−4718

surface-confined redox voltammetry of HLM. The ratio between the reduction and oxidation peak currents was close to unity. Integration of the peak area provided the charge (Q) in coulombs (Table 1).[22] The formal potentials of HLM

Table 1. Electrochemical Parameters of Liver Microsomal Films Adsorbed on Different Carbon Electrode Materials under Nitrogen Atmosphere

film type	$E^{o\prime}$/V vs Ag/AgCl	Q/nC	PWHM/mV	$\Delta E^{o\prime}$/pH mV	k_s (s^{-1})
GC/HLM	−0.45 (±0.01)	33 ± 2	63 ± 4	72 ± 6	91 ± 11
HPG/HLM	−0. 45 (±0.005)	330 ± 58	68 ± 2	64 ± 5	61 ± 4
EPG/HLM	−0.45 (±0.01)	347 ± 20	82 ± 2	57 ± 6	36 ± 4
BPG/HLM	−0.47 (±0.005)	232 ± 20	74 ± 4	75 ± 8	29 ± 5

physisorbed on BPG, EPG, GC, and HPG electrodes did not change significantly. However, the electroactive amounts (proportional to the measured charge) of microsomal films among the surface defective EPG and HPG electrodes were comparable to each other, and about 10-times greater than the smooth GC electrode and about 1.5-times greater than the moderately defective BPG electrode (Table 1).

The positive shifts in formal potentials with decreasing pH suggest the occurrence of proton-coupled ET processes (involving equal numbers of electrons and protons, Table 1) in the microsomal films on different carbon electrodes. The average shift in formal potentials per pH unit (tested pH conditions: pH 5.5, 6.5, and 7.5) was close to the Nernstian 59 mV pH^{-1} for the HPG/HLM and EPG/HLM films and higher than 59 mV for the GC/HLM and BPG/HLM films (Table 1).[14] The peak width at half-maximum (PWHM) was in the range of 63−82 mV for all microsomal films (Table 1). This range is between the ideal 90.6 and 45.3 mV for one electron and two electron processes, respectively.[22]

Prior studies showed that FAD can accept up to two electrons from NADPH, whereas FMN acts as a one electron carrier to reduce CYPs in the biocatalytic pathway.[3,4,35] The observed lower PWHM values of liver microsomal films are similar to that reported for rat liver microsomes in layer-by-layer films with polyions (∼ −0.45 V vs Ag/AgCl, pH 7.0, PWHM 70 ± 8 mV).[14] For purified human CPR in surfactant films (∼ −0.47 V vs Ag/AgCl, pH 8.0) that exhibited a PWHM of 70 mV, a multielectron transfer process was inferred.[31] On the basis of our results and the reported literature, we suggest the possibility for a one electron process or a mixed one and two electron transfer processes taking place in the direct electrochemistry of the designed microsomal films. Overall, the examined electrochemical properties suggest the nonideal surface voltammetry of liver microsomal proteins.

Electrode-dependent Electron Transfer Kinetics. From the increase in peak separation with scan rates (Figure 2C) that was subtracted for the nonzero constant peak separation at low scan rates (≤100 mV s^{-1}), similar to other reported studies,[33,36−38] we determined the direct ET rate constants (k_s, s^{-1})[39] of microsomal films on the BPG, EPG, GC, and HPG disk electrodes (Table 1). The resulting fit of peak separation with the Butler−Volmer surface voltammetry showed good agreement (Figure S5).[33,38,39]

The direct ET rate of the microsomal film on the smooth GC electrode was 2.5−3.0 times greater than that of the microsomal films on the BPG and EPG electrodes and 1.5-times greater than that of the microsomal film on the HPG electrode (Table 1). The magnitudes of electroactive coverage and ET rates suggest that electrode roughness and surface defects favor enhanced amounts of electroactive microsomal proteins (e.g., HPG and EPG), while a flat and surface defect-free GC surface seems to allow HLM molecules to orient in a uniform manner with a net fast ET rate (Figure 1, SEM images). Figure 2C shows that the greater peak separation of microsomal films in the respective electrodes with increasing scan rates correlates inversely with the determined rates of direct ET (Table 1), as per the Butler−Volmer surface voltammetry.[39]

Film Thickness and Electrochemical Kinetics. Spectral reflectance measurements illustrated that the nominal range of dry film thicknesses of microsomal films on the defective EPG and HPG electrodes was greater than that of the smooth GC and less defective BPG electrodes as presented in Table 2. The

Table 2. Thickness Data of the Immobilized Microsomal Films on Different Electrodes

film type	dry film thickness (μm)
GC/HLM	0.3−1.3
HPG/HLM	5.0−10.0
EPG/HLM	2.0−8.5
BPG/HLM	0.2−3.0

upper limits of dry film thicknesses of HLM among electrodes qualitatively correlated with the measured extent of electroactive amounts (Table 1). In contrast, significant differences were observed in the kinetics of ET and film stability among the microsomal films on the different electrodes. For example, GC/HLM and BPG/HLM films of similar thicknesses displayed the highest and lowest direct ET rates, respectively. A similar feature is also reflected in the k_s values among the EPG/HLM and HPG/HLM electrodes (Tables 1 and 2).

The absence of correlation between film thickness and ET kinetics suggests the need to consider electrode factors such as surface defects, roughness, geometry, and chemical groups that can influence the secondary interactions between the electrode and the phospholipid membranes of HLM (Figure 1 and further discussion below on XPS analysis). These in turn can alter the orientations of membrane-bound oxidoreductases and metabolic enzymes with respect to electrode. Hence, the pathway of ET between electrode and membrane-bound microsomal proteins appears to be the underlying factor in controlling electrochemical kinetics.

Surface Properties and Connection to Electrochemical Rates. The surface characteristics of polished electrodes were determined by XPS analysis as shown in Figure 3. Results show that the GC surface contains the highest oxygen content and the BPG surface with the lowest oxygen content, and the reverse is observed with regard to carbon levels. EPG and HPG surfaces consist of intermediate oxygen levels and carbon content close to the BPG (Table 3). The determined percentage values of C and O composition are in agreement with the reported literature on polished graphite and glassy carbon surfaces.[40−43]

Surface oxygen density can be related to the extent of polarity and the surface carbon levels to the extent of

DOI: 10.1021/ac5044362
Anal. Chem. 2015, 87, 4712−4718

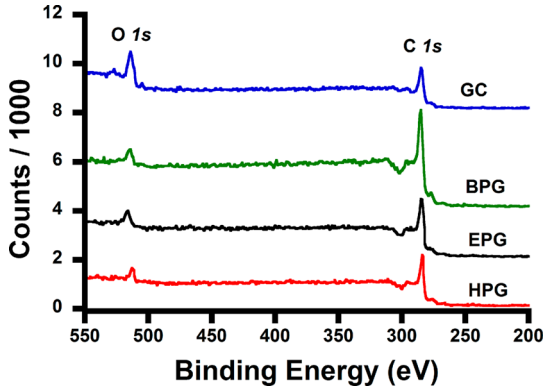

Figure 3. XPS spectra of polished electrode surfaces.

Table 3. Carbon and Oxygen Levels of Four Carbon Electrodes

electrode	carbon	oxygen
GC	77%	23%
HPG	91%	9%
EPG	89%	11%
BPG	94%	6%

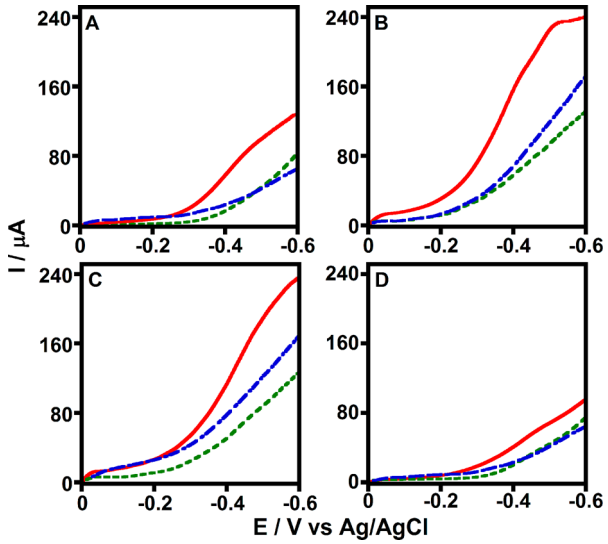

Figure 4. Cyclic voltammograms of microsomal films (red), phospholipid films (blue), and bare electrodes (green) of (A) GC, (B) HPG, (C) EPG, and (D) BPG electrodes in 0.9 mM oxygen concentration. Experimental conditions: stirred pH 7.0 phosphate buffer, 0.15 M NaCl, 25 °C, scan rate 0.3 V s^{-1}.

hydrophobicity. The flat/smooth surface (Figures 1A) of GC is ascribed to enable uniform HLM layer arrangement (with homogeneous protein orientation), and the highly polar nature (Table 3) is attributed to favor faster charge transfer kinetics in a relatively thinner film of HLM on GC over other electrodes. On the other hand, the less polar nature of BPG with an irregular surface appears to have varying interactions with the phospholipid membranes of HLM and cause mixed orientations of microsomal proteins in the film, resulting in slower ET rates. HPG and EPG electrodes with intermediate levels of oxygen functionalities with respect to BPG and GC, and with extensive surface defects, showed ET rate constants falling between BPG and GC.

Taken together, this study finds that surface oxygen density of a carbon electrode influences charge transports in the phospholipid membranes of immobilized HLM. It is important to note that the electron transfer rate constants determined are representative of the whole film of HLM on a given electrode and are not controlled by one specific electrode property due to the complexity of interactions between an electrode and HLM as against a simple purified protein system.

Electroactive Microsomal Film Stability on Electrodes. The electroactive stability of microsomal films on BPG, EPG, GC, and HPG electrodes was monitored by cycling the potential continuously between 0 and −0.6 V vs Ag/AgCl for 200 cycles (scan rate 0.1 V s^{-1}) in an anaerobic pH 7.0 buffer. The GC/HLM film retained ∼30% of the initial current. The HPG/HLM and EPG/HLM films retained about 85% of initial currents, and the BPG/HLM film retained about ∼50% of the initial current. This level of electroactive HLM stability after 200 cycles on the HPG and EPG electrodes is likely satisfactory for electrocatalytic and biosensing applications.

Electrochemical O_2 Binding Kinetics to HLM. Oxygen is required in CYP-catalyzed monooxygenase activity to form the active CYP-heme oxidant, which can subsequently transfer the reactive oxygen to oxidize a bound substrate.[4,18] For oxygen to bind CYPs, the Fe^{III}-heme of CYP needs to be reduced first to the Fe^{II}-heme-CYP form (a one e^- reduction). Figure 4 (solid curve in red) shows the catalytic cyclic voltammograms of oxygen reduction currents by microsomal films on the various carbon electrodes. The relative magnitudes of oxygen reduction currents among the designed microsomal films were in the following order: HPG/HLM ≈ EPG/HLM > GC/HLM > BPG/HLM.

The cyclic voltammograms of polished bare electrodes or those adsorbed with a phospholipid layer in the absence of immobilized microsomes did not show the characteristic enzyme-mediated electrocatalytic oxygen reduction (Figure 4, broken curves) but rather displayed small reduction currents at more negative onset potentials that were due to direct oxygen reduction at carbon electrodes. This result confirms the specific role of microsomal heme proteins in catalyzing oxygen reduction that appears to be facilitated by electron donation from electrode-reduced CPR molecules (Figure 2A). It is also possible that microsomal cyt b_5-heme may undergo reduction by the electrode-reduced CPR. However, this reduction process in the presence of vesicles (as the case for microsomes) has been shown to be slow and less favorable.[44]

Oxygen reduction currents by microsomal proteins on electrodes were analyzed by Lineweaver−Burk kinetics (Figure 5) to obtain the apparent Michaelis−Menten affinity constant (K_M) of each microsomal film.[45] Estimated apparent K_M values among four electrodes were in the range of 0.5−1.0 mM, which is not appreciably different. A possible reason could be the observed reductase-like direct electrochemistry of HLM (Figure 2A), and as a result indirect oxygen binding to reductase-reduced heme proteins in HLM films is not directly influenced by the type of electrode used.

Electrocatalytic Testosterone Hydroxylation and CYP-specific Inhibition. We investigated the biocatalytic activity of liver microsomal films by monitoring the conversion of testosterone to 6*β*-hydroxytestosterone via bulk electrolysis at an applied constant potential of −0.6 V vs Ag/AgCl followed by HPLC detection of the product. Among several CYP enzymes, the CYP 2C9, 2C19, and 3A4 present in HLM have been shown to play roles in catalyzing the testosterone

DOI: 10.1021/ac5044362
Anal. Chem. 2015, 87, 4712−4718

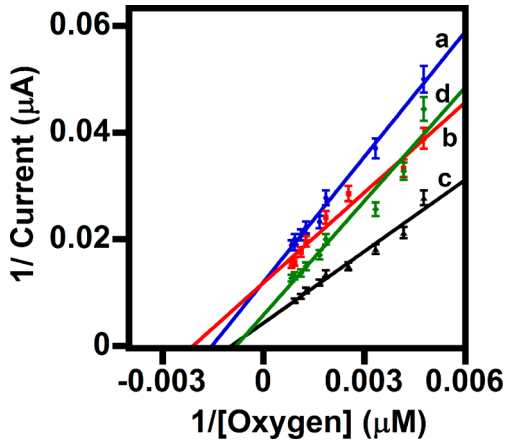

Figure 5. Lineweaver–Burk plots for oxygen reduction currents versus oxygen concentration for (a) GC/HLM, (b) HPG/HLM, (c) EPG/HLM, and (d) BPG/HLM electrodes. Experimental conditions: stirred phosphate buffer, pH 7.0, scan rate 0.3 V s^{-1}, 25 °C.

hydroxylation.[46] For the electrolysis study, we chose the catalytically superior and relatively more stable HPG/HLM film as an optimal electrode system identified. After electrolysis, the reaction mixture was analyzed by HPLC, and the hydroxylation product was identified using the standard 6β-hydroxytestosterone (Figures 6a and S7).

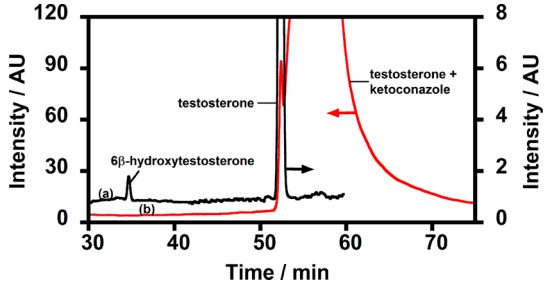

Figure 6. HPLC chromatograms of reaction mixture after 1 h of electrolysis of HPG/HLM electrodes at −0.6 V vs Ag/AgCl under a constant oxygen supply at 25 °C, pH 7.0: (a) 250 μM testosterone; (b) 250 μM testosterone + 100 μM ketoconazole.

To determine whether the testosterone hydroxylation by the HPG/HLM film was catalyzed by CYPs, the reaction was performed in the presence of ketoconazole, a potent inhibitor of CYP activity toward testosterone hydroxylation.[16] Figure 6b shows that ketoconazole inhibited the CYP-catalyzed formation of 6β-hydroxytestosterone. The observed biocatalytic property indicates that HLM directly adsorbed on HPG can facilitate electron transfer from electrode to CPR to CYPs and retain the bioactivity of bound CYPs. Moreover, we confirmed that the polished bare HPG electrode in the absence of HLM did not catalyze the testosterone hydroxylation (Figure S6). Figure S7 provides the chromatograms of 6β-hydroxytestosterone standard and ketoconazole inhibitor.

CONCLUSIONS

The results presented demonstrate the feasibility of designing a one-step, rapid microsomal bioreactor on optimal HPG or EPG electrodes for biocatalytic applications. Film thickness of HLM, stability, and electroactive protein amounts are controlled by the extent of electrode surface defects, while the rate of ET is controlled by the combined effects of surface oxygen functionalities and surface flatness of electrodes. Considering the importance of human liver microsomes in pharmaceutical drug development and toxicology fields, the presented method to simplify the microsomal bioelectrode design is suggested to be useful for inexpensive drug metabolism and inhibition assays. We envision that the new findings of this study will have notable significance in the design of modern one step liver microsomal electrodes for rapid electrochemical biosensing and biocatalytic applications.

ASSOCIATED CONTENT

Supporting Information

Figures S1–S7 for UV–vis absorbance, FTIR characterization, N_2 and CO CVs of HLM, peak current vs scan rate plots, experimental peak separations with Butler–Volmer surface voltammetry fit, chromatogram of polished HPG electrolysis reaction mixture in 250 μM testosterone and saturated oxygen, and chromatograms of 6β-hydroxytestosterone standard and ketoconazole inhibitor. This material is available free of charge via the Internet at http://pubs.acs.org

AUTHOR INFORMATION

Corresponding Author

*E-mail: gopan.krishnan@okstate.edu.

Author Contributions

C.W. and R.N. contributed equally to this work.

Notes

The authors declare no competing financial interest.

ACKNOWLEDGMENTS

We are grateful for the financial support by Oklahoma State University.

REFERENCES

(1) Krishnan, S.; Rusling, J. F. Thin Iron Heme Enzyme Films on Electrodes and Nanoparticles for Biocatalysis. In *New and Future Developments in Catalysis*; Suib, S. L., Ed.; Elsevier Publishers, 2013; Chapter 5, pp 125–147.
(2) O'Reilly, E.; Kohler, V.; Flitsch, S. L.; Turner, N. J. *Chem. Commun.* **2011**, *47*, 2490–2501.
(3) Guengerich, F. P. *J. Biochem. Mol. Toxicol.* **2007**, *21*, 163–168.
(4) Ortiz de Montellano, P. R. *Cytochrome P450*; Kluwer/Plenum: New York, 2005.
(5) Gutierrez, A.; Grunau, A.; Paine, M.; Munro, A. W.; Wolf, C. R.; Roberts, G. C. K.; Scrutton, N. S. *Biochem. Soc. Trans.* **2003**, *31*, 497–501.
(6) Johnson, E. F.; Connick, J. P.; Reed, J. R.; Backes, W. L.; Desai, M. C.; Xu, L.; Estrada, D. F.; Laurence, J. S.; Scott, E. E. *Drug Metab. Dispos.* **2014**, *42*, 9–22.
(7) Krishnan, S.; Schenkman, J. B.; Rusling, J. F. *J. Phys. Chem. B* **2011**, *115*, 8371–8380.
(8) Das, A.; Sligar, S. G. *Biochemistry* **2009**, *48*, 12104–12112.
(9) Krishnan, S.; Walgama, C. *Anal. Chem.* **2013**, *85*, 11420–11426.
(10) Walgama, C.; Krishnan, S. *J. Electrochem. Soc.* **2014**, *161*, H47–H52.
(11) Nerimetla, R.; Walgama, C.; Ramanathan, R.; Krishnan, S. *Electroanalysis* **2014**, *26*, 675–678.
(12) Wienkers, L. C.; Heath, T. G. *Nat. Rev. Drug Discovery* **2005**, *4*, 825–833.
(13) Sultana, N.; Schenkman, J. B.; Rusling, J. F. *J. Am. Chem. Soc.* **2005**, *127*, 13460–13461.
(14) Krishnan, S.; Rusling, J. F. *Electrochem. Commun.* **2007**, *9*, 2359–2363.

DOI: 10.1021/ac5044362
Anal. Chem. 2015, 87, 4712–4718

(15) Wasalathanthri, D. P.; Malla, S.; Faria, R. C.; Rusling, J. F. *Electroanalysis* **2012**, *24*, 2049−2052.
(16) Mie, Y.; Suzuki, M.; Komatsu, Y. *J. Am. Chem. Soc.* **2009**, *131*, 6646−6647.
(17) Krishnan, S.; Wasalathanthri, D.; Zhao, L.; Schenkman, J. B.; Rusling, J. F. *J. Am. Chem. Soc.* **2011**, *133*, 1459−1465.
(18) Guengerich, F. P.; Martin, M. V.; Sohl, C. D.; Cheng, Q. *Nat. Protoc.* **2009**, *4*, 1245−1251.
(19) Banks, C. E.; Compton, R. G. *Analyst* **2006**, *131*, 15−21.
(20) Stewart, J. C. *Anal. Biochem.* **1980**, *104*, 10−14.
(21) Samoc, A.; Miniewicz, A.; Samoc, M.; Grote, J. G. *J. Appl. Polym. Sci.* **2007**, *105*, 236−245.
(22) Bard, A.; Faulkner, L. R. In *Electrochemical Methods: Fundamentals and Applications*, 2nd ed.; Wiley: Hoboken, NJ, 2001.
(23) Sander, R. *Compilation of Henry's Law Constants for Inorganic and Organic Species of Potential Importance in Environmental Chemistry*, Version 3, 1999. Available at www.henrys-law.org.
(24) Cracknell, J. A.; Wait, A. F.; Lenz, O.; Friedrich, B.; Armstrong, F. A. *Proc. Natl. Acad. Sci. U. S. A.* **2009**, *106*, 20681−20686.
(25) Goñi, F. M.; Arrondo, J. L. R. *Faraday Discuss. Chem. Soc.* **1986**, *81*, 117−126.
(26) Beng, G.; Pop, V. I.; Ionescu, M.; Hodârnău, A.; Tilinca, R.; Frangopol, P. T. *Biochim. Biophys. Acta* **1983**, *750*, 194−199.
(27) Rice, R. J.; Pontikos, N. M.; McCreery, R. L. *J. Am. Chem. Soc.* **1990**, *112*, 4617−4622.
(28) Blanford, C. F.; Armstrong, F. A. *J. Solid State Electrochem.* **2006**, *10*, 826−832.
(29) Huang, H.; Hu, N.; Zeng, Y.; Zhou, G. *Anal. Biochem.* **2002**, *308*, 141−151.
(30) Xiao, L.; Dickinson, E. J. F.; Wildgoose, G. G.; Compton, R. G. *Electroanalysis* **2010**, *22*, 269−276.
(31) Shukla, A.; Gillam, E. M. J.; Bernhardt, P. V. *Electrochem. Commun.* **2006**, *8*, 1845−1849.
(32) Sultana, N.; Schenkman, J. B.; Rusling, J. F. *Electroanalysis* **2007**, *19*, 2499−2506.
(33) Krishnan, S.; Abeykoon, A.; Schenkman, J. B.; Rusling, J. F. *J. Am. Chem. Soc.* **2009**, *131*, 16215−16224.
(34) Aono, T.; Sakamoto, Y.; Miura, M.; Takeuchi, F.; Hori, H.; Tsubaki, M. *J. Biomed. Sci.* **2010**, *17*, 90.
(35) Evans, J. P.; Xu, F.; Sirisawad, M.; Miller, R.; Naumovski, L.; Ortiz de Montellano, P. R. *Mol. Pharmacol.* **2007**, *71*, 193−200.
(36) Razzaq, H.; Qureshi, R.; Schiffrin, D. J. *Electrochem. Commun.* **2014**, *39*, 9−11.
(37) Ghanem, M. A.; Chrétien, J.-M.; Pinczewska, A.; Kilburn, J. D.; Bartlett, P. N. *J. Mater. Chem.* **2008**, *18*, 4917−4927.
(38) Munge, B.; Das, S. K.; Ilagan, R.; Pendon, Z.; Yang, J.; Frank, H. A.; Rusling, J. F. *J. Am. Chem. Soc.* **2003**, *125*, 12457−12463.
(39) Laviron, E. *J. Electroanal. Chem.* **1979**, *101*, 19−28.
(40) Wang, Y.; Cao, J.; Zhou, Y.; Ouyang, J.-H.; Jia, D.; Guo, L. *J. Electrochem. Soc.* **2012**, *159*, A579−A583.
(41) Wei, L.; Wu, F.; Shi, D.; Hu, C.; Li, X.; Yuan, W.; Wang, J.; Zhao, J.; Geng, H.; Wei, H.; Wang, Y.; Hu, N.; Zhang, Y. *Sci. Rep.* **2013**, *3*, 2636.
(42) Brunetti, B.; De Giglio, E.; Cafagna, D.; Desimoni, E. *Surf. Interface Anal.* **2012**, *44*, 491−496.
(43) Chen, P.; McCreery, R. L. *Anal. Chem.* **1996**, *68*, 3958−3965.
(44) Guengerich, F. P. *Arch. Biochem. Biophys.* **2005**, *440*, 204−211.
(45) Kim, E. J.; Amorelli, B.; Abdo, M.; Thomas, C. J.; Love, D. C.; Knapp, S.; Hanover, J. A. *J. Am. Chem. Soc.* **2007**, *129*, 14854−14855.
(46) Yamazaki, H.; Shimada, T. *Arch. Biochem. Biophys.* **1997**, *346*, 161−169.

DOI: 10.1021/ac5044362
Anal. Chem. 2015, 87, 4712−4718